Case II diffusion: effect of solvent molecule size

Thomas P. Gall*, Ronald C. Lasky* and Edward J. Kramer†
Department of Materials Science and Engineering, and the Materials Science Center, Bard Hall, Cornell University, Ithaca, NY 14853, USA
(Received 20 June 1989; accepted 9 September 1989)

Rutherford back-scattering spectrometry has been used to examine the detailed composition vs. depth profile for polystyrene exposed at 25°C to the vapour (activity = 0.45) of a series of 1-iodo-n-alkanes ranging from iodopropane ($n=3$) to iodooctane ($n=8$), where n is the number of carbon atoms on the alkane chain. All the iodoalkanes tested exhibit case II diffusion. The velocity V of the case II front decreases exponentially with n. The diffusion coefficient D in the glass, which is determined from the concentration profile of the iodoalkanes ahead of the front using the measured value of V, decreases exponentially with increasing n; D decreases by approximately a factor of 4 for each carbon atom added to the alkane chain. These data are compared with previous studies, which show that D decreases exponentially with the molecular diameter d, calculated from the density of the pure liquid solvent: $D=D_0\,e^{-\delta d}$, where δ is a constant for spherically symmetric solvent molecules. For the linear iodoalkanes D shows a similar exponential decrease but with a 20% lower value of δ, resulting in D for these non-spherical molecules being as much as three orders of magnitude larger than that for spherical molecules with an equivalent d. At the critical concentration ϕ_c for case II diffusion to begin, the swelling rate $d\phi/dt$ at the surface of the sample also decreases approximately exponentially with increasing n. The swelling rate decreases strongly with the osmotic pressure P_{os}, while P_{os} at ϕ_c decreases with the molecular volume (and thus with n). The change in $d\phi/dt$ with n, inferred from the corresponding change in P_{os}, can account for nearly all of the observed dependence of $d\phi/dt$ on n. The Thomas and Windle model of case II diffusion leads to the following prediction for V: $V=[(D/\phi_c)(d\phi/dt)|_{\phi_c}]^{1/2}$. We find that the front velocities derived from this equation using the measured values of D and $(d\phi/dt)|_{\phi_c}$ are in quantitative agreement with the experimental values of V for the entire series of iodoalkanes, a result that provides strong confirmation of the Thomas and Windle model.

(Keywords: case II diffusion; surface swelling; induction time; Rutherford back-scattering spectrometry)

INTRODUCTION

For organic solvents that swell glassy polymers significantly, an extreme situation, known as case II diffusion[1], can occur. In case II diffusion, the solvent volume fraction at the surface ϕ_s increases until a critical concentration ϕ_c is reached at the surface, at which time the case II front forms and moves into the polymer at a constant velocity[2–5]. The first attempts at models of case II diffusion used variable material properties[6–8], or two-stage diffusion[9–11], but were not able to explain the constant velocity V of the case II front. Crank's[7] introduction of the swelling stress of the solvent into the diffusion equations gave the first in a series of quantitative models[12–18] that led to the Thomas and Windle[19–23] (TW) model of case II diffusion. For a summary of the development of models of case II diffusion, see Lasky[24]. The TW model predicts linear kinetics and a sharp diffusion front, and allows one to predict quantitatively the magnitude of V.

The TW model of case II diffusion, which treats the swelling of the polymer as an osmotic-pressure-driven deformation, can be used to derive an equation[25] to predict V. As the polymer absorbs solvent, the swelling rate $d\phi/dt$ ahead of the case II front is a function f of the osmotic pressure P_{os} and the volume fraction of solvent ϕ:

$$d\phi/dt = f(P_{os}, \phi) \tag{1}$$

The difference in the chemical potential of the solvent from the local equilibrium value, which gives rise to P_{os}, can, for a solution in which the activity of the solvent is proportional to ϕ, be expressed as the natural logarithm of the ratio of the local equilibrium solvent volume fraction. Therefore P_{os} is approximated by:

$$P_{os} \simeq \frac{k_B T}{\Omega} \ln\left(\frac{\phi_{eq}}{\phi}\right) \tag{2}$$

where k_B is Boltzmann's constant, T is the absolute temperature, Ω is the solvent molecular volume and ϕ_{eq} is a local equilibrium value of the solvent volume fraction.

Once the case II front has formed, the concentration of diffusant in the front stays relatively constant, so the case II front acts as a moving boundary of nearly constant concentration. For a reference frame moving with the case II front, the conditions ahead of the front approach steady state. For flat samples where the diffusion distance is small compared with the size of the sample, the diffusion equation can be solved in one dimension. For steady-state diffusion described by a diffusion coefficient D ahead of a boundary moving with a constant velocity

* Present address: IBM Endicott, Endicott, NY 13760, USA
† To whom correspondence should be addressed

0032-3861/90/081491-09

V, Fick's second law can be written:

$$\frac{\partial \phi}{\partial t} = \frac{\partial}{\partial x}\left(D\frac{\partial \phi}{\partial x} + V\phi\right) = 0 \tag{3}$$

where t is time and x is distance ahead of the boundary. For a case II diffusion front, the solution for the Fickian precursor ahead of the front, if D is not a function of solvent concentration, is[12]:

$$\phi = \phi_c \exp(-Vx/D) \tag{4}$$

Taking the derivative of equation (2) with respect to x, and substituting equation (4) for ϕ_{eq} gives:

$$\frac{dP_{os}}{dx} = -\frac{k_B T}{\Omega}\left(\frac{V}{D} + \frac{d \ln \phi}{dx}\right) \tag{5}$$

For the steady-state conditions ahead of the front, the derivative of ϕ with distance can be converted to a time derivative, and near the front P_{os} will go through a maximum, such that at this maximum:

$$0 = -\frac{k_B T}{\Omega}\left(\frac{V}{D} - \frac{1}{\phi V}\frac{d\phi}{dt}\right) \tag{6}$$

Assuming that the osmotic-pressure maximum is sufficiently close to the front so that the parameters can be evaluated at ϕ_c gives[26]:

$$V = \left[\left(\frac{D}{\phi_c}\right)\left.\frac{d\phi}{dt}\right|_{\phi_c}\right]^{1/2} \tag{7}$$

To avoid the need for simplifying assumptions about the polymer swelling rate, an experimentally measured swelling rate is used to calculate V.

While in their model Thomas and Windle use an oversimplified relationship for the swelling rate[19] shown in equation (1) (they assume that the swelling rate is linear in P_{os} and exponentially dependent on ϕ), the use of Rutherford back-scattering spectrometry (RBS) will allow us to measure directly $d\phi/dt$, ϕ_c, D and V independently. These experimental values will be used to test equation (7) directly for a series of 1-iodo-n-alkanes.

The data for D and $d\phi/dt$ will also be used to investigate how diffusion and swelling vary with solvent molecular size. Previous data[27] for D have been correlated to the molecular diameter d of the solvent calculated from the solvent density as a pure liquid. The experimental values of D for linear iodoalkanes will be compared with those of solvents of similar density.

EXPERIMENTAL PROCEDURE

Sample preparation and exposure to solvents

The polymer used in this study was monodisperse polystyrene (PS) with a molecular weight of 390 000, which was purchased from Pressure Chemical Co. Films about 20 μm thick were prepared from a 12% by weight solution of the polystyrene in toluene either by dipping a substrate into the solution, or by evaporating drops of the solution on a substrate. The films were dried for 4 h, then annealed in a vacuum oven at 125°C for 1 h. The samples were aged at 50°C for one day in order to minimize the amount of physical ageing due to varying storage times at room temperature.

The samples were exposed to solvent vapours in flasks that had a solution of iodoalkane solvent and polystyrene in the bottom. The volume fraction of solvent in the solution determines the partial pressure of the solvent vapour in the flask. The volume fraction ϕ of solvent in the solution was held constant throughout these experiments at 0.20 (0.45 vapour activity). The solvents used ranged from iodopropane to iodooctane. The molecular volume Ω of the solvent used to estimate ϕ was calculated from the density of the pure liquid at 20°C. The polystyrene samples were first brought to the same temperature as the vapour, then suspended vertically in the flask, well away from the flask walls. Calculations[28] show that the reduction in the activity of the iodoalkane at the surface of the sample due to vapour transport effects, and depletion of the iodoalkane from the vapour, will be negligible for the experimental conditions used in this study. The temperature of the flask was controlled to ± 0.1°C by immersing the sample flask in a water bath.

After the samples were removed from the solvent flask they were immediately immersed in liquid nitrogen to freeze the concentration profile in place. The dewar of liquid nitrogen was kept within 10 cm of the sample so that transfer times of under 1 s could be achieved. All subsequent handling of the samples until they were in the RBS vacuum chamber was done under the liquid nitrogen, or in a glove bag filled with dry nitrogen, to prevent water vapour from condensing on the surface of the sample during the rapid transfer from the liquid nitrogen to the vacuum chamber load lock. The sample stage in the RBS vacuum chamber was also cooled with liquid nitrogen to freeze the solvent molecules in place and to minimize the effect of radiation damage caused by the ion beam on the measured concentration profile.

Rutherford back-scattering analysis of the concentration profile

The volume fraction vs. depth profile of the iodoalkane solvent can be measured using Rutherford back-scattering spectrometry (RBS)[26]. A 2.4 MeV beam of $^4He^{2+}$ ions is focused to a 2 mm square spot on the PS sample. A small number of ions are back-scattered elastically from nuclei in the sample and are recorded by an energy-sensitive detector. *Figure 1a* shows a typical spectrum of the yield vs. energy of the ions scattered through an angle of 170° from a polystyrene sample containing iodopentane. The spectrum can be converted to ϕ vs. depth of the solvent (see *Figure 1b*) if the densities, scattering cross-sections and ion energy-loss rates are known.

The solvents used all contain iodine, an ideal tag for RBS of hydrocarbon samples because of the large difference in nuclear mass between the heavy iodine tag and the light carbon nuclei of the hydrocarbon polymer. The energy of a recoiling alpha particle increases with the mass of the target nucleus, so the large difference in nuclear mass gives a wide separation between the energy of $^4He^{2+}$ ions back-scattered from iodine and carbon nuclei.

The back-scattered ions lose energy due to inelastic interactions with electrons in the sample, and this energy loss can be used to calculate the depth at which the scattering event occurred. The larger the energy difference between ions back-scattered from the heavy nuclear tag and the polymer, the deeper one can analyse the sample before the $^4He^{2+}$ ions scattered from the tag nucleus overlap with those scattered from carbon at the surface. The energy and yield of $^4He^{2+}$ ions scattered from iodine atoms in a polystyrene sample can be used to calculate

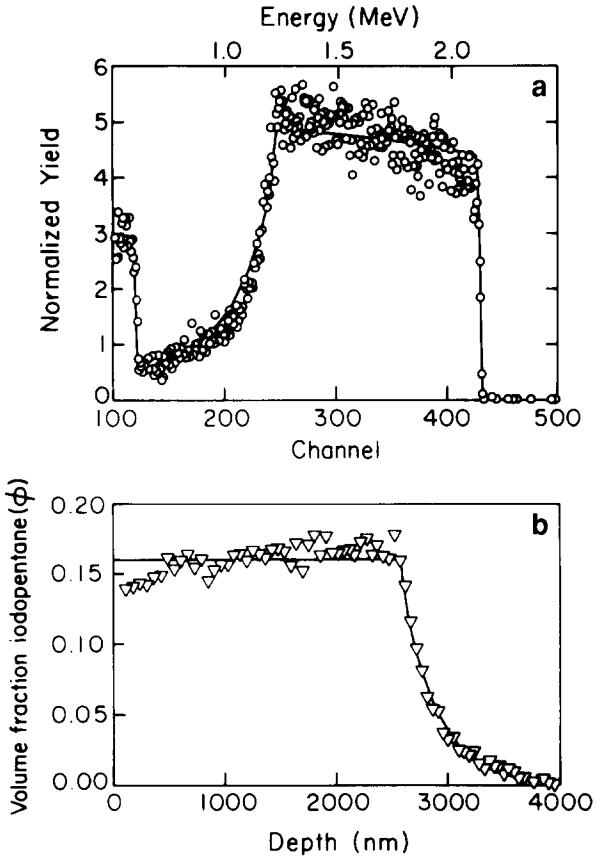

Figure 1 (a) RBS spectrum of PS sample exposed to 0.45 activity iodopentane for 20 h at 25°C. (b) Volume fraction vs. depth profile derived from the data in part (a)

the volume fraction vs. depth of the solvent molecules with a resolution of 50 nm up to a depth of 4 μm.

Since the scattering cross-sections and the rate of energy loss of the ions vary with energy, the interpretation of the spectrum was performed by modelling the sample as a series of thin layers. A computer algorithm[29] was used to calculate a simulated back-scattering yield vs. energy curve for the sample. The case II front depth, atomic fraction of iodine and the diffusion coefficient are found by fitting simulated RBS spectra to the experimental data.

Experimental results

The shape of the volume fraction ϕ vs. depth profile in *Figure 1b* shows the characteristics of case II diffusion. The volume fraction of solvent behind the case II front is constant to within the resolution of the RBS (except where some solvent is lost at the surface during the transfer from the flask to the liquid nitrogen) and drops off sharply ahead of the case II front, as is shown in *Figure 1*. Ahead of the front there is a Fickian precursor in which the volume fraction of solvent decreases approximately exponentially with depth. Measuring the front depth for a series of samples exposed to the iodoalkane solvent for varying times gives a linear increase in front depth with time, as is shown in *Figure 2*. The slope of *Figure 2* is the front velocity V and the intercept on the abscissa is the induction time t_i for case II diffusion to begin.

Once the critical volume fraction for case II diffusion has been reached, the polymer behind the front converts to a mobile material. The diffusion coefficient of a solvent in a high-mobility phase is orders of magnitude higher than for a glassy polymer, so any additional solvent absorbed after the case II front forms moves rapidly inwards to the front. The volume fraction of solvent at the surface is constrained by the relatively slow motion of the polymer chains, so the surface volume fraction ϕ_s does not increase rapidly with time.

Figure 3 shows volume fraction vs. depth data for samples exposed to 0.45 activity iodopentane vapour for varying times; the full curves are simulated RBS spectra, which were fitted to the experimental data, then converted

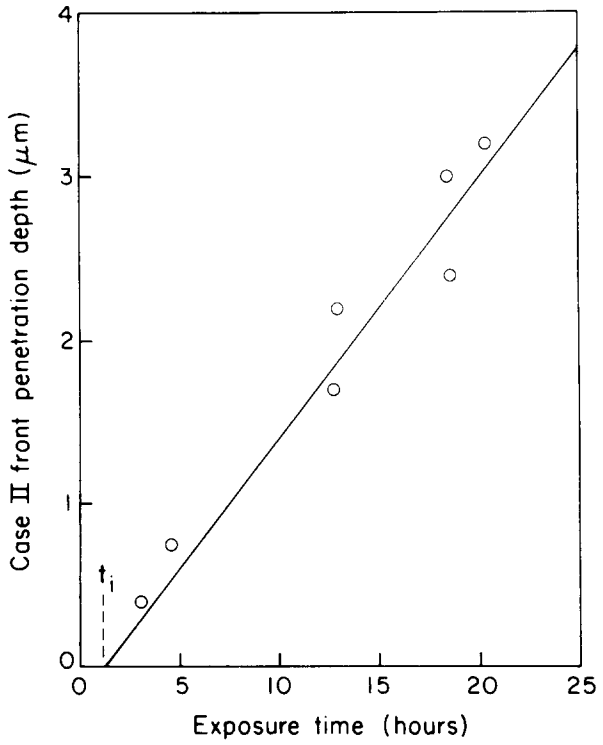

Figure 2 The case II front depth vs. time for PS samples exposed to 0.45 activity iodopentane at 25°C. The full line is a linear least-squares fit

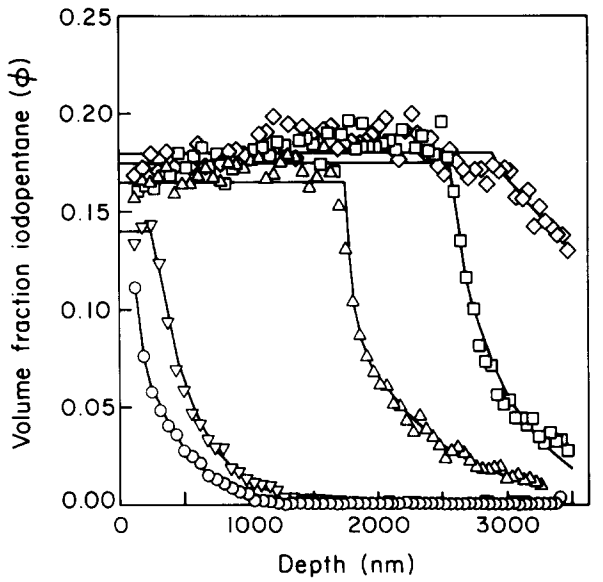

Figure 3 A family of volume fraction vs. depth curves for case II diffusion of 0.45 activity iodopentane into PS at 25°C for: (○) 7200 s, (▽) 10 980 s, (△) 66 280 s, (□) 73 020 s, (◇) 175 860 s. The full curves are derived from simulations of the data

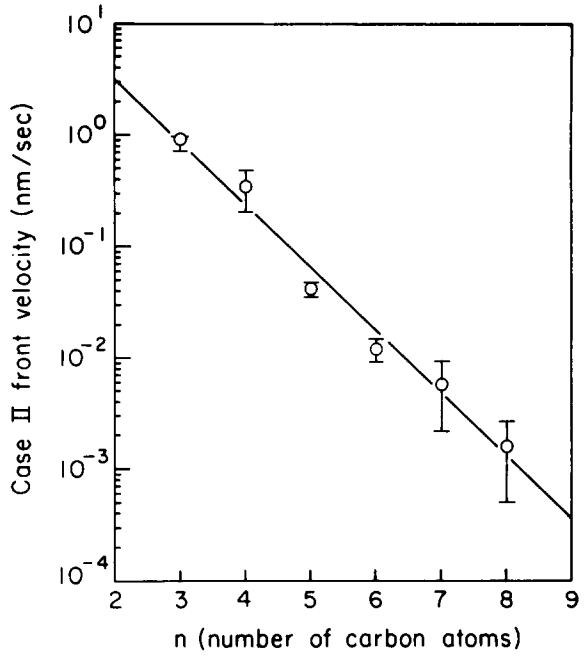

Figure 4 The logarithm of the case II front velocity vs. number of carbon atoms in the alkane chain for an iodoalkane solvent at 0.45 activity and 25°C. The full line is a linear least-squares fit

to volume fraction vs. depth. For times less than t_i the volume fraction profile is a smoothly decreasing function approximating that expected for Fickian diffusion with a constant surface concentration. For longer times, when ϕ_s reaches ϕ_c, the case II front forms. The case II front is a sharp boundary that forms between the outer mobile phase and the inner glassy polymer; the front position is marked by a sharp drop in ϕ as is shown in *Figure 3*. Once formed, the case II front moves inwards with a constant velocity V.

Figure 4 shows V vs. the number n of carbon atoms in the alkane chain. For a constant equilibrium volume fraction of solvent ϕ_{eq}, the case II front velocity decreases exponentially with n. The front velocities shown in *Figure 4* were calculated from the front depth vs. time of several different samples. The 95% confidence limits for V (shown as error bars in *Figure 4*) are calculated from the sum of the squared residuals to the least-squares fit to the case II front depth vs. exposure time plots.

For diffusion ahead of the case II front, the constant front volume fraction and velocity lead to a steady-state condition in a coordinate system moving with the front. The calculation of D takes advantage of a simple solution to Fick's second law for diffusion ahead of a moving boundary, shown in equation (4). A simulated RBS spectrum for the volume fraction profile calculated from equation (4) is matched to the experimental RBS spectrum ahead of the front to calculate D.

To obtain the data required to fit to equation (4), ϕ vs. x is found from the RBS spectrum, and the value of V is found from a front depth vs. time plot such as *Figure 2*. The examples of simulated RBS spectra corresponding to different values of D in *Figure 5* show the sensitivity of the fit to D. The D giving the best fit for iodoheptane shown in *Figure 5* is $2.7 \times 10^{-14}\,cm^2\,s^{-1}$ and was found by an optimization algorithm[30]. Values of D vs. n shown in *Figure 6* were obtained by fitting equation (4) to the same RBS data used to calculate V in *Figure 4*. The fitting routine calculates a standard deviation from the fit, but the variation in sample preparation and exposure produces larger variations in the measured value of D, so the 95% confidence limits for D shown as error bars in *Figure 6* were calculated from the variation among the values of D measured for successive samples.

Also plotted in *Figure 6* is the value of n^2D. Previous measurements of the diffusion of a dry-film photoresist[31] appeared to show n^2D approaching a constant at higher n values, inviting the speculation that the higher-n solvents were beginning to diffuse by a reptation-like mechanism in the glassy photoresist. (D should scale as n^{-2} for simple reptation.) The present experiments show no hint of such a levelling-off in n^2D and thus provide no evidence for a simple reptation-like mechanism in the

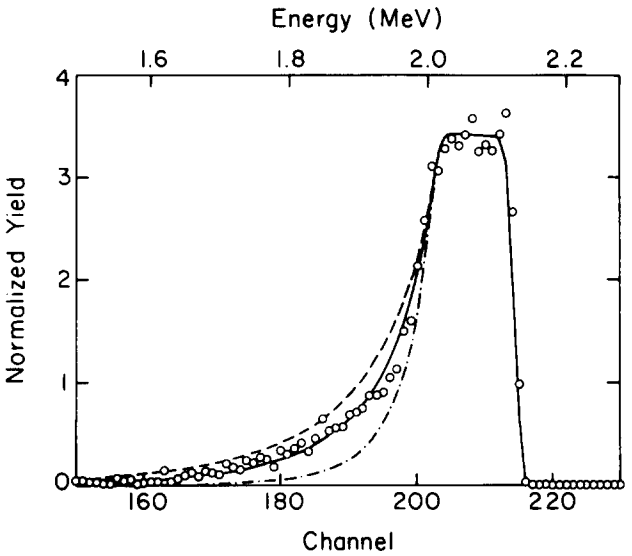

Figure 5 RBS spectrum of 0.45 activity iodoheptane diffusion into PS for 191 100 s at 25°C, and simulated spectra. D is varied for each simulation to show the sensitivity of the fit to the value of D: (——) $D = 2.68 \times 10^{-14}\,cm^2\,s^{-1}$, (– – –) $D = 3.5 \times 10^{-14}\,cm^2\,s^{-1}$, (— · —) $D = 1.5 \times 10^{-14}\,cm^2\,s^{-1}$

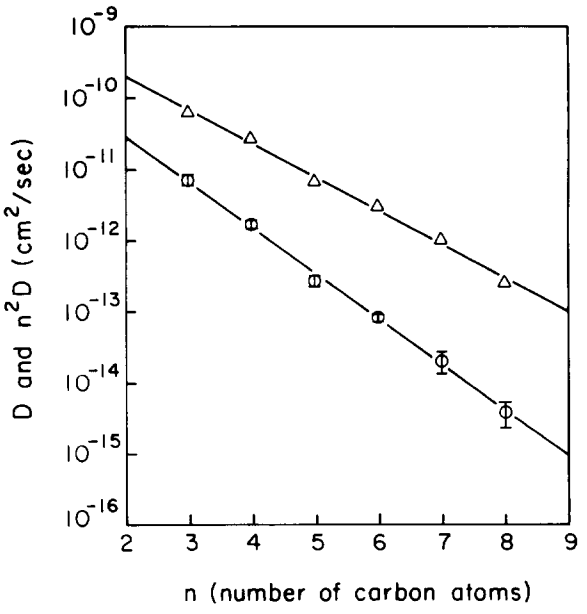

Figure 6 The logarithm of D (○) and n^2D (△) vs. number of carbon atoms in the alkane chain for samples exposed to 0.45 activity iodoalkanes at 25°C. The full lines are linear least-squares fits

glass. As shown elsewhere[28], however, a mechanism can still exist where the molecule moves more easily along its length than normal to it. In a glassy polymer, unlike the melt, the reptation-like mechanism does not give a simple power-law decrease in D with molecular length.

Figure 7 shows the induction time t_i vs. n for the series of iodoalkanes; t_i is determined from the intercept of the front depth vs. time plots as indicated above. The value of the volume fraction of solvent at the surface ϕ_s, evaluated at t_i, is the critical volume fraction for case II diffusion to begin, ϕ_c. The volume fraction vs. depth data

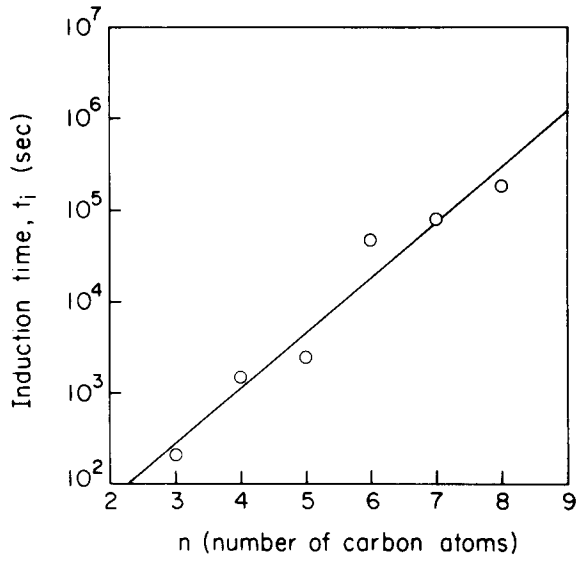

Figure 7 The induction time for case II diffusion t_i vs. number of carbon atoms in the alkane chain for PS samples exposed to 0.45 activity iodoalkanes at 25°C. The full line is a linear least-squares fit

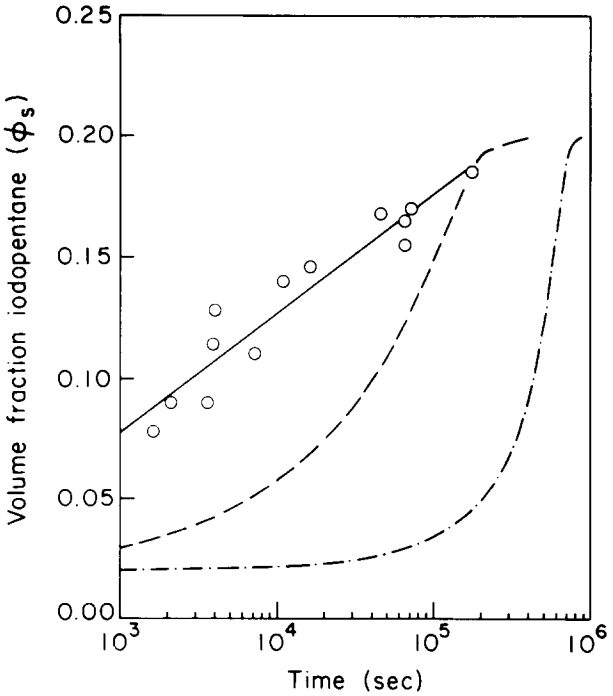

Figure 8 Solvent volume fraction at the surface ϕ_s vs. log time for PS samples exposed to 0.45 activity ($\phi_{eq}=0.2$) iodopentane at 25°C. The full line is a linear least-squares fit to the data. The broken curve is calculated from an equation by Lasky, and the chain curve is from the TW model

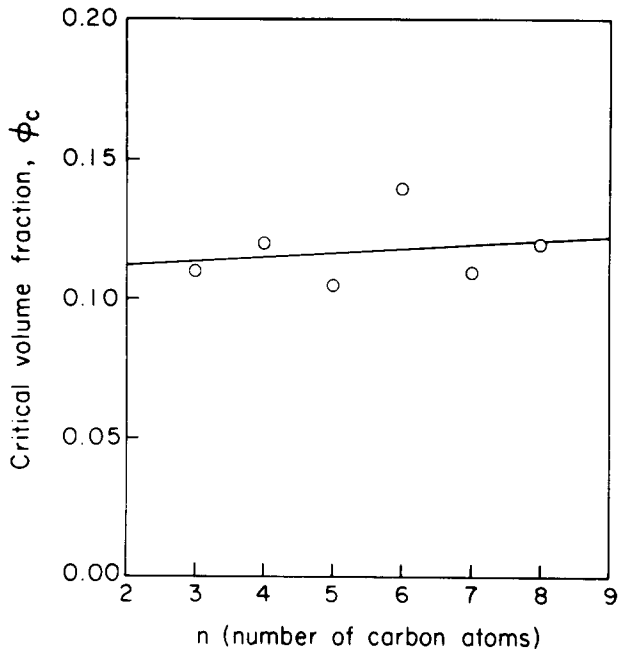

Figure 9 The critical volume fraction for case II diffusion ϕ_c vs. the number of carbon atoms in the alkane chain for PS samples exposed to 0.45 activity iodoalkanes at 25°C. The full line is a linear least-squares fit

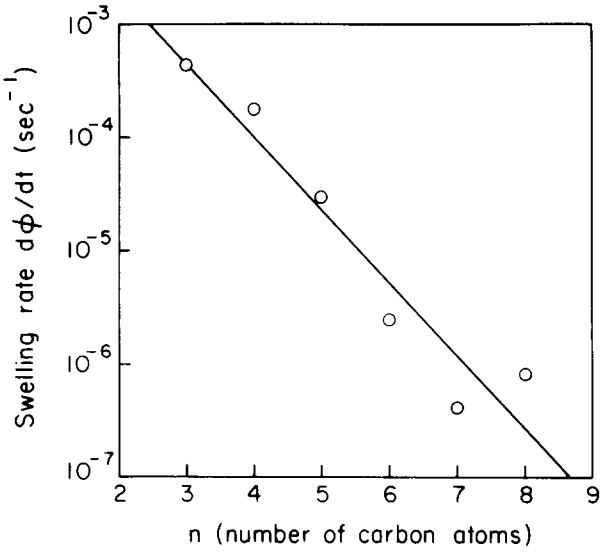

Figure 10 Swelling rate vs. number of carbon atoms in the alkane chain for PS samples exposed to 0.45 activity iodoalkane vapour at 25°C. The full line is a linear least-squares fit

in *Figure 3* can be used to determine ϕ_s, and ϕ_c can be found from plots of ϕ_s vs. log t typified by *Figure 8*. Values of ϕ_c found by the above procedure are shown in *Figure 9*; these values do not deviate significantly from $\phi_c=0.12$ over the entire series of iodoalkanes.

The swelling rate $d\phi/dt$ of the polymer at the critical volume fraction can also be determined from ϕ_s vs. log t data such as those shown in *Figure 8*. The critical swelling rate so obtained decreases by over three orders of magnitude as n increases from 3 (iodopropane) to 8 (iodooctane) as shown in *Figure 10*. As discussed below, most of this decrease is due to the decrease in osmotic pressure P_{os} that accompanies the increase in molecular volume Ω as n increases.

DISCUSSION

Prediction of V using the Thomas and Windle model

The Thomas and Windle model of case II diffusion was used to derive an equation to predict the case II front velocity (equation (7), repeated here for convenience):

$$V=\left[\left(\frac{D}{\phi_c}\right)\left.\frac{d\phi}{dt}\right|_{\phi_c}\right]^{1/2}$$

Equation (7) is valid when measured values of D and swelling rate are used, even though the assumptions used in the original TW model for the dependence of swelling rate on P_{os}, or for that matter for the dependence of D on ϕ, are not experimentally correct. The measured values of the critical swelling rate $d\phi/dt$ at ϕ_c from *Figure 10*, the diffusion coefficient D from *Figure 6* and ϕ_c from *Figure 9* are used in equation (7) to predict values of the front velocity V for the entire series of iodoalkanes. These predicted values of V are compared with the experimentally measured values in *Figure 11*. The agreement between the predicted and measured values of V is excellent. That this prediction succeeds for all of the iodoalkanes tested constitutes a strong confirmation of the basic ideas behind the Thomas and Windle model of case II diffusion. Having shown that D and $d\phi/dt$ determine V, these variables will be discussed in more detail.

The change in polymer swelling rate with solvent molecular size

The remarkable decrease in the critical swelling rate with solvent molecular size shown in *Figure 10* needs to be explained. Since we measure the local volume fraction at the surface as a function of time, these changes cannot be attributed to the observed decrease in the diffusion coefficient. Rather they must be intrinsic to the swelling process itself. Since the critical volume fraction ϕ_c remains roughly constant as the solvent molecular size increases, it seems most unlikely that these large changes in swelling rate can be due to changes in the plasticizing ability of the solvent as its size increases. The possibility remains that the decrease in swelling rate is due to the decrease in osmotic pressure P_{os} at ϕ_c as a result of the increase in molecular volume Ω; from equation (2) P_{os} at ϕ_c depends inversely on Ω, viz.:

$$P_{os}(\phi_c)=\frac{k_BT}{\Omega}\ln\left(\frac{\phi_{eq}}{\phi_c}\right) \quad (8)$$

If this explanation is to be believed, however, the critical swelling rate must be the very strong function of P_{os} shown in *Figure 12*.

In *Figure 12* the osmotic pressure has been computed using equation (8) and the solvent molecular volumes. The data can be described by a power-law dependence of the form:

$$(d\phi/dt)|_{\phi_c}=K[P_{os}(\phi_c)]^{\kappa} \quad (9)$$

where $\kappa\simeq 12$ and K is a constant. Support for this steep dependence of swelling rate on osmotic pressure can be found in the experiments of Lasky[24], where he exposed polystyrene samples to various vapour activities of iodohexane and measured the front velocity V and diffusion coefficient D using identical techniques to those used here. (Lasky also attempted to measure the surface swelling rate, but we now believe his measured rates to be somewhat low relative to the correct values due to contamination of his surface by a film of oxidized hydrocarbon oil from the oil bath used to anneal the samples. Subsequent experiments[32] have shown that only the surface swelling was affected by this contamination; both V and D were unaffected.)

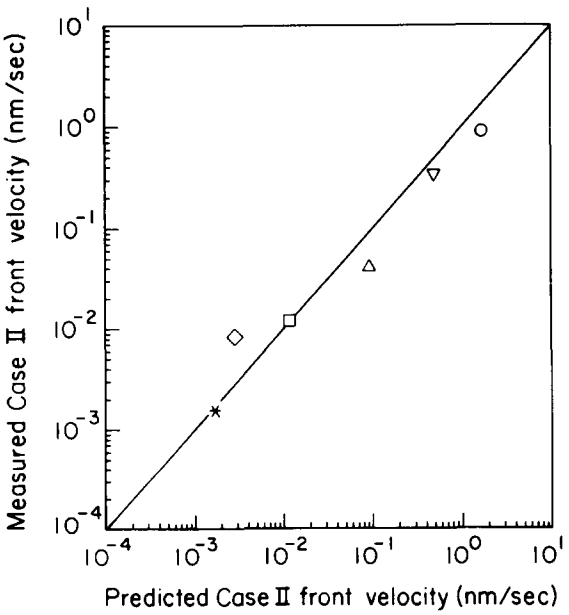

Figure 11 The logarithm of measured vs. predicted case II front velocities for iodoalkane solvents at 0.45 activity and 25°C: (○) iodopropane, (▽) iodobutane, (△) iodopentane, (□) iodohexane, (◇) iodoheptane, (*) iodooctane. The full line indicates equal predicted and measured velocities

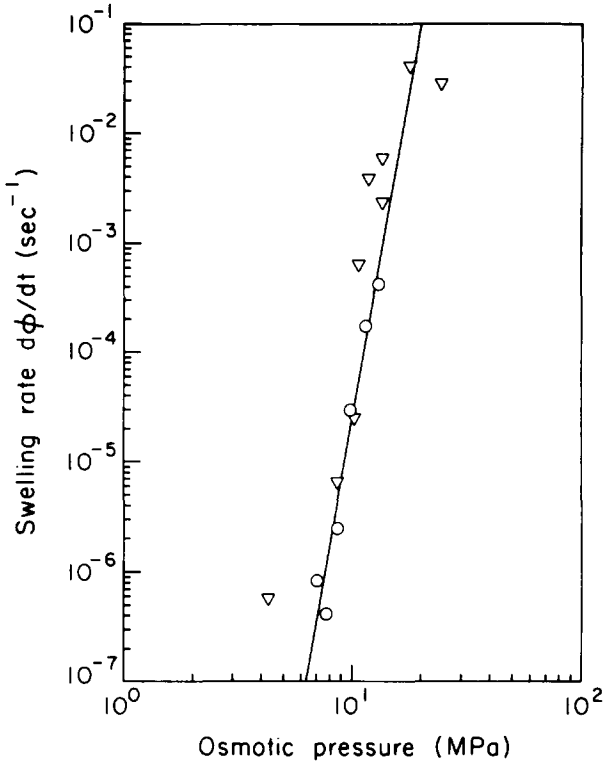

Figure 12 Swelling rate at $\phi_c=0.12$ vs. P_{os} for PS samples exposed at 25°C: (○) 0.45 activity iodoalkanes with n ranging from 2 to 8; and (▽) calculated swelling rates from Lasky's data for various solvent activities of iodohexane ranging from 0.20 to 0.66. The full line is a linear least-squares fit

Inserting Lasky's values of D and V, corrected for vapour transport effects[28], into equation (7), we can estimate values of the critical swelling rate $d\phi/dt|_{\phi_c}$ at different values of ϕ_{eq}, and thus at the different values of P_{os} used in his experiments. (Just as we found that ϕ_c was approximately independent of n, Lasky found that ϕ_c was approximately independent of ϕ_{eq}.) The values of $d\phi/dt$ calculated from Lasky's data are also plotted, as inverted triangles, in *Figure 12*. The strong power-law dependence of $d\phi/dt$ on P_{os} of equation (9) is also an excellent description of the increase of the critical swelling rate due to the increase in iodoalkane activity in Lasky's experiments.

Equation (9) is quite different from the original linear viscous swelling law proposed by Thomas and Windle ($d\phi/dt \sim P_{os}$) and the non-linear viscous swelling rate ($d\phi/dt \sim P_{os}^{2.2}$) proposed by Lasky *et al.*[33] for low vapour activities. The difference can be further emphasized by using the linear viscous and non-linear viscous swelling laws as outlined by Lasky *et al.* to predict the surface swelling rate as a function of time. These predictions, which are shown as the chain and broken curves respectively in *Figure 8*, predict swelling kinetics that are several orders of magnitude slower than those actually observed.

The failure of either the linear viscous or simple non-linear viscous models to describe the swelling rate, which is essentially a complex mechanical property of the plasticized (by solvent) glassy polymer, should not be surprising to anyone familiar with the mechanical properties of polymer glasses; similar models cannot adequately describe the strain rate at high stress of even unplasticized glassy polymers. To emphasize this point we plot, in *Figure 13*, the yield stress σ_y of polystyrene plasticized by a certain volume fraction ϕ of small molecules (calculated by Lasky[24] using data from Kambour[34]), as well as P_{os} vs. solvent volume fraction computed from equation (2) for several molecular volumes corresponding to iodopropane, iodopentane and iodooctane at an equilibrium volume fraction ϕ_{eq} of 0.20 corresponding to a vapour activity of 0.45. The osmotic pressure is not extrapolated to the very high values corresponding to low solvent volume fractions since there will always be a small volume fraction of holes, or free volume (estimated by Lasky to be 0.02 for polystyrene at 25°C), which can be filled by the solvent without deforming the polymer chains and evoking an osmotic-pressure resistance. Lasky[24] has constructed a similar plot for several vapour activities corresponding to his iodohexane exposures.

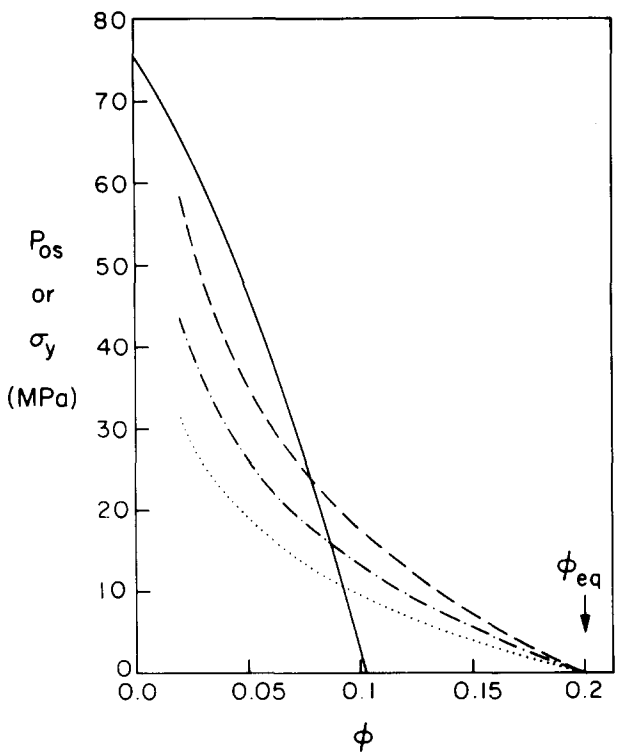

Figure 13 A graph of the yield stress σ_y of PS (——)[24] and P_{os} vs. ϕ at $\phi_{eq}=0.20$ for (– – –) iodopropane, (— · —) iodopentane and (· · ·) iodooctane at 25°C

Note that for all the iodoalkanes at $\phi_{eq}=0.20$, the osmotic pressure is below the yield stress until $\phi \sim 0.1$ is reached and then it exceeds the yield stress. The ϕ value where the crossing takes place is reasonably close to the observed value of ϕ_c. Moreover, the osmotic pressure at the crossing is always greater than 10 MPa, i.e. a yield-like mechanical phenomenon can be expected. The yielding in the case of solvent swelling is caused by physicochemical forces (the osmotic pressure) rather than purely mechanical forces. In this analogy the volume fraction ϕ corresponds to the strain ε and the swelling rate $d\phi/dt$ corresponds to the strain rate $d\varepsilon/dt$. The dependence of $P_{os}(\phi_c)$ on $d\phi/dt$ is thus analogous to the dependence of the yield stress on the strain rate. It is well known for glassy polymers in general[35], and polystyrene in particular[36], that the dependence of the yield stress on strain rate is weak and is well represented by a power law of the form:

$$\sigma_y = \sigma_{y0}(d\varepsilon/dt)^{1/k} \qquad (10)$$

where σ_{y0} is a constant and k is between 10 and 20. Thus the magnitude of the analogous exponent κ, which describes the osmotic-pressure dependence of the swelling rate, seems reasonable if we regard the onset of case II diffusion (the critical condition) as a chemically driven yielding of the glassy polymer.

This analogy between the onset of case II diffusion and yielding also explains some additional recent observations that are difficult to reconcile with the conventional view that case II diffusion starts when the T_g of the plasticized polymer at the surface drops below the ambient temperature. Recent observations[37,38] on diffusion of solvents into polyimides show that case II diffusion starts in these cases under high-osmotic-pressure conditions even though the glass transition temperature of the polyimide is not decreased to the experimental temperature. The natural explanation is that the high osmotic pressure of the solvent causes the polyimide (which has a relatively low yield stress normal to the surface[37]) to 'yield' and thus case II diffusion to begin. If this explanation is correct, the increase in D that accompanies the start of case II diffusion is a consequence of the 'yielding' and not simply a plasticization effect. It is significant that large increases in D have been observed[39,40] as a result of mechanical yielding. Presumably the increase in polymer molecular mobility in the yielding state causes the large increase in D observed. Case II diffusion can then be viewed as fundamentally caused by a large increase in D induced by a chemically driven yielding of the polymer.

In support of the yielding analogy it is also useful to note that, in the case of the polyimides, where the material

behind the case II front is below T_g, there is a small gradient of concentration behind the front corresponding to a diffusion coefficient[38] there of 4×10^{-12} cm^2 s^{-1} rather than the value $> 10^{-8}$ cm^2 s^{-1} that can be inferred from the absence of a measurable gradient of the iodoalkanes in polystyrene[24]. In polystyrene, the swollen polymer behind the front is a rubber-like phase (above T_g) and the solvent has a high diffusion coefficient, while in polyimide the swollen layer remains glassy (below T_g) and so the solvent diffusion coefficient remains relatively low.

The dependence of D on molecular size and shape

For the diffusion of organic solvents into glassy polymers at very low diffusant concentrations, there are reports in the literature[27,41] of linear flexible molecules having a higher diffusion coefficient than isomers limited to a fixed shape. Berens[41] compared D for spherical molecules in polystyrene to D for elongated molecules in polystyrene. *Figure 14* shows that when D is plotted vs. average molecular diameter d (calculated from liquid densities), the values for elongated molecules fall above the line through the points for spherical molecules. *Figure 14* also shows D for iodoalkanes superimposed on Berens' data. The iodoalkanes also fall above the fit to the spherical molecules, and a fit to D for iodoalkanes has a smaller slope. The ratio of the slope of the log D vs. d curve for iodoalkanes to that of spherical molecules from *Figure 14* is 0.8. The lower value of the slope for iodoalkanes suggests that the effective cross-section of the molecule for performing a jump depends on a diameter smaller than the average diameter, which is reasonable for a molecule that can take on elongated shapes.

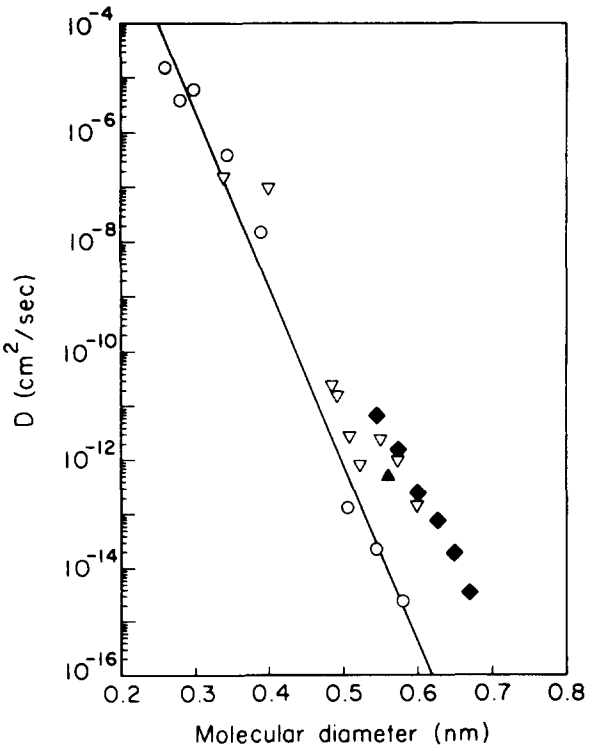

Figure 14 Diffusion coefficient vs. molecular diameter at 25°C: (○) spherical molecules[27], (▽) non-spherical molecules[27], (◆) iodoalkanes and (▲) deuterated toluene[28]. The full line is a linear least-squares fit to D for spherical molecules

CONCLUSIONS

The series of 1-iodo-n-alkanes ranging from iodopropane ($n=3$) to iodooctane ($n=8$) show case II diffusion in PS at 25°C with the front velocity decreasing exponentially with n.

The case II front velocity for iodoalkanes can be quantitatively predicted from:

$$V = \left[\left(\frac{D}{\phi_c} \right) \left. \frac{d\phi}{dt} \right|_{\phi_c} \right]^{1/2}$$

where D is the diffusion coefficient measured ahead of the front and $d\phi/dt$ is the empirical swelling rate of the glass at the critical concentration for case II diffusion. That this prediction succeeds for all of the iodoalkanes tested constitutes a strong confirmation of the fundamental principles of the Thomas and Windle model.

Case II diffusion can be interpreted as a yielding phenomenon of the polymer due to the osmotic pressure of the solvent. The polymer swelling rate, which is analogous to a mechanical strain rate, is determined by the osmotic stress applied to the polymer.

The diffusion coefficient of the iodoalkanes in the region ahead of the front also decreases exponentially with n, but the rate of decrease is not as large as that of solvent molecules with a spherical shape. The lower rate of decrease of D with n indicates that the effective cross-sectional area of the molecule for making a translational jump is reduced for molecules that can twist into elongated shapes.

ACKNOWLEDGEMENTS

Primary support by the US Army Research Office (Durham) is gratefully acknowledged. We also benefited from the use of the facilities of the Materials Science Centre at Cornell University, which is funded by the NSF-DMR-MRL program. T. P. Gall and R. C. Lasky received fellowship support from the IBM resident study program. We greatly appreciate the enthusiastic guidance of Professor J. W. Mayer on all aspects of Rutherford back-scattering spectrometry.

REFERENCES

1 Alfrey, T. *Chem. Eng. News* 1965, **43**, 64
2 Hartley, G. S. *Trans. Faraday Soc.* (*B*) 1964, **42**, 6
3 Robinson, C. *Trans. Faraday Soc.* (*B*) 1964, **42**, 12
4 Thomas, N. L. and Windle, A. H. *Polymer* 1978, **19**, 255
5 Hartley, G. S. *Trans. Faraday Soc.* 1949, **47**, 820
6 Crank, J. and Park, G. S. *Trans. Faraday Soc.* 1951, **47**, 1072
7 Crank, J. *J. Polym. Sci.* 1953, **11**, 151
8 Park, G. S. *J. Polym. Sci.* 1953, **11**, 97
9 Bagley, E. and Long, F. A. *J. Am. Chem. Soc.* 1955, **77**, 2172
10 Newns, A. C. *Trans. Faraday Soc.* 1956, **52**, 1533
11 Long, F. A. and Richmond, D. *J. Am. Chem. Soc.* 1960, **82**, 513
12 Peterlin, A. *J. Polym. Sci.* (*B*) 1965, **3**, 1083
13 Peterlin, A. *Makromol. Chem.* 1969, **124**, 136
14 Petropoulos, J. H. and Rousis, P. P. *J. Chem. Phys.* 1967, **47**, 1491
15 Petropoulos, J. H. and Rousis, P. P. *J. Polym. Sci.* (*C*) 1969, **22**, 917
16 Petropoulos, J. H. and Rousis, P. P. in 'Permeability of Plastic Films and Coatings', (Ed. H. B. Hopfenberg), Plenum, New York, 1974
17 Astarita, G. and Sarti, G. *Polym. Eng. Sci.* 1978, **18**, 388
18 Sarti, G. *Polymer* 1979, **20**, 827
19 Thomas, N. L. and Windle, A. H. *Polymer* 1982, **23**, 529
20 Thomas, N. L. and Windle, A. H. *Polymer* 1977, **18**, 1195
21 Thomas, N. L. and Windle, A. H. *J. Membr. Sci.* 1978, **3**, 337

22 Thomas, N. L. and Windle, A. H. *Polymer* 1980, **21**, 619
23 Thomas, N. L. and Windle, A. H. *Polymer* 1981, **22**, 627
24 Lasky, R. C. PhD Thesis, Cornell University, 1986
25 Hui, C. Y., Wu, K. C., Lasky, R. C. and Kramer, E. J. *J. Appl. Phys.* 1987, **61**, 5129
26 Mills, P. J., Palmstrom, C. J. and Kramer, E. J. *J. Mater. Sci.* 1986, **21**, 1479
27 Berens, A. R. and Hopfenberg, H. B. *J. Membr. Sci.* 1982, **10**, 283
28 Gall, T. P. PhD Thesis, Cornell University, 1989
29 Doolittle, L. R. *Nucl. Instrum. Meth.* (*B*) 1985, **9**, 334
30 Doolittle, L. R. *Nucl. Instrum. Meth.* (*B*) 1986, **15**, 227
31 Mills, P. J. and Kramer, E. J. *J. Mater. Sci.* 1986, **21**, 4151
32 Ognjanovic, R. unpublished
33 Lasky, R. C., Kramer, E. J. and Hui, C. Y. *Polymer* 1988, **29**, 673
34 Kambour, R. J. Proc. Int. Conf. Mech. Environ. Sensitive Cracking Materials, University of Surrey, April 1977
35 Young, R. J. 'Introduction to Polymers', Chapman and Hall, London, 1981, p. 267
36 Brady, T. E. and Yeh, G. S. Y. *J. Appl. Phys.* 1971, **42**, 4622
37 Gattiglia, E. and Russell, T. P. *J. Polym. Sci., Polym. Phys. Edn.* 1989, **27**, 2131
38 Kramer, E. J. unpublished
39 Harmon, J. P., Lee, S. and Li, J. C. M. *J. Polym. Sci., Polym. Chem. Edn.* 1987, **25**, 3215
40 Miller, P. and Kramer, E. J. *J. Mater. Sci.* in press
41 Berens, A. R. IUPAC Conf. Proc., 1982, p. 737